NANOSYSTEMS: PHYSICS, CHEMISTRY, MATHEMATICS, 2020, 11 (5), P. 519–528

Influence of complexing agent, pH of solution and thickness on morphological and optical properties of ZnS particles layer prepared by electrochemical deposition technique

Jitendra Borse[1], Arun Garde[2]

[1]Department of Physics, Late Pushpadevi Patil Arts & Science College, Risod 444506, India
[2]Department of Physics, SPH Arts, Science and Commerce College, Nampur 423204, India

jaborse@gmail.com, arungarde@yahoo.co.in

DOI 10.17586/2220-8054-2020-11-5-519-528

Zinc sulfide particles layer were grown on FTO glass and stainless steel substrates by electrode position technique from aqueous solution that contained 0.1 N zinc sulfate, 0.1 N sodium thiosulfate and 0.1 N triethanolamine was used as complexing agent. The deposing potential was analyzed by cyclic voltammetry technique. The ZnS particle growth was studied in the range of deposition time from 10 to 40 minutes. The thickness of layer was found to be the highest, 3.92 μm, at 20 min. The various percentage of complexing agent, pH of solution and thicknesses of film were characterized by scanning electron microscope (SEM) and UV-Visible spectrophotometer. The effects of complexing agent, pH of solution and thickness of layer on morphological and optical properties of ZnS were investigated. The Electrical resistivity of ZnS was found thickness dependent. The Chemical Composition of ZnS particles analysed by EDAX (Energy Dispersive Analysis by X-ray).

Keywords: complexing agent, electrodeposition, pH of bath, resistivity, thickness of ZnS particles layer.

Received: 14 May 2020

Revised: 29 May 2020

Final revision: 21 September 2020

1. Introduction

The research of chalcogenide semiconductor materials for solar energy conversion and other related photovoltaic applications has been recently initiated. ZnS belongs to group II–VI semiconductor material. It has cubic and hexagonal crystal structure [1]. It is semiconductor material with a large band gap greater than 3.5 eV [2]. ZnS films have been prepared by using various techniques such as electrochemical deposition, chemical bath deposition,spray pyrolysis [3]. Amongst these various deposition methods,electrochemical deposition is more attractive, being a simple, low temperature and inexpensive technique. The prepared films have been widely used in variety of application such as window layer of solar cell, laser materials, sensors, photoconductors, anti-reflection coating [4]. The Chalcogenide semiconductor material show unique optical behavior due to quantum size effect and widely studied because of their applications in optoelectronic devices [5]. The ZnS material is suitable as a window layer in hetero junction photovoltaic solar cells [6–10]. In this research, we have reported deposition of ZnS film on stainless steel substrate by an electrode position technique [11, 12]. The main aim of this research is to study the effect of triethanolamine as complexing agent and pH of bath on the morphological and optical properties of ZnS material respectively.

2. Method

ZnS particles were deposited on stainless steel substrate by an electrochemical deposition technique shown in Fig. 1. The type of AISI 316 stainless steel plate/FTO glass was used as the working electrode with graphite as the counter electrode and Ag/AgCl working as reference electrode to measured deposing potential of ZnS with respect to working electrode. All the precursors were used for the deposition as AR grade. Zinc sulfide particles layer were electrode posited on to the stainless steel substrate for 10 to 40 min at room temperature from a solution containing 0.1 N Zinc sulfate($ZnSO_4$), 0.1 N sodium thiosulfate ($Na_2S_2O_3$) at pH = 3.5. The 0.1 N solution of triethanolamine (TEA) was added in bath as complexing agent. The role of complexing agent to formation of complex stoichiometric compound of Zn and S ions and substrate is fully covered. The cyclic voltammetry technique was used to study the electrochemical property such as deposing potential of ZnS materials. The stainless steel substrates of 2.25 cm^2 dimension area were cleaned by acetone and distilled water before deposition. The distance between the working electrode and counter electrode was kept constant as 1 cm during deposition of materials. The ZnS particles are formed on the stainless steel substrate according to reaction. This is electrochemical reaction of thiosulfate ion. The process of disproportionate of $S_2O_3^{2-}$ to S and SO_3^{2-} is possible,

$$S_2O_3^{2-} \longrightarrow S + SO_3^{2-}. \quad (1)$$

Zinc ions are involved in reduction and oxidation reaction with transfer of two electrons

$$Zn^{+2} + 2e^{-} + S \longrightarrow ZnS. \tag{2}$$

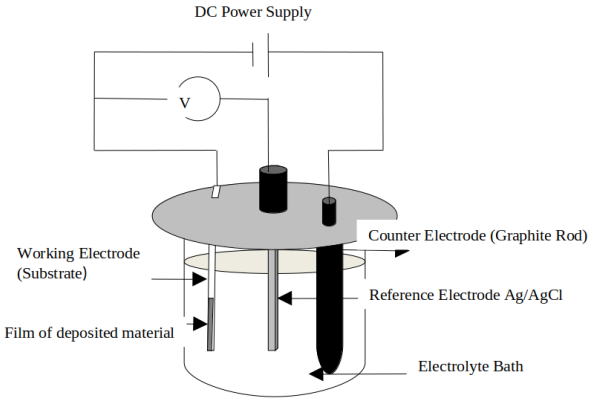

FIG. 1. Electrochemical deposition set-up for deposition of ZnS particles layer

The formation of ZnS material according to reaction (2).

The electrical parameters such as DC voltage and current density were adjusted at 1700 mV and 4.4 mA/cm^2 respectively. The zinc sulfidefilms were prepared at deposition time (10 to 40 min) and thickness of layer studied [13]. The pH of electrolyte bath was adjusted from 3.5 to 5 by adding 0.1 N sodium hydroxide(NaOH). The ZnS films were prepared at different percentage of 0.1 N triethanolamine (TEA). The layer of ZnS was further characterized by UV-Visible spectrophotometer. Energy dispersive analysis by X-ray diffraction (EDAX) and Scanning electron microscopy (SEM). The chemical bonding of functional groups was analysed by FT-IR technique. The electrical resistivity of ZnS was estimated by two point probe method.

3. Result and discussion

3.1. Energy dispersive analysis by X-ray spectroscopy

Figure 2 shows energy dispersive analysis by X-ray spectroscopy of ZnS particles. It showed the elemental composition for the Zn and S ions in the sample. The ZnS particles were shown to be deposited successfully. The EDX spectrum in Fig. 3 revealed that as grown layer composed of only Zn and S species. The At% ratio of Zn, S and O was found 62.48, 6.76 and 30.76 respectively.

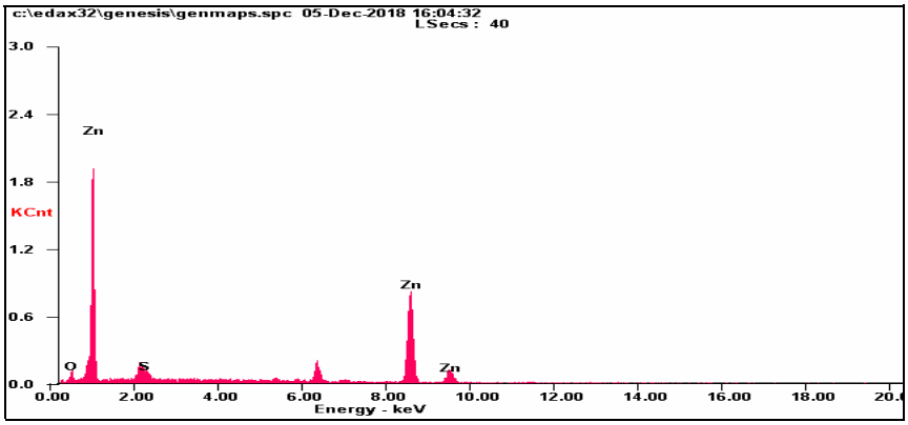

FIG. 2. Energy dispersive analysis of ZnS particles

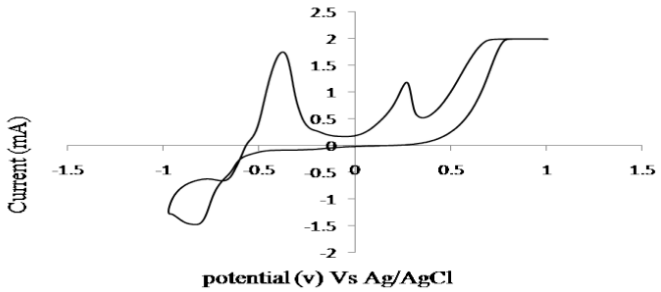

FIG. 3. Cyclic voltammetry of measured current versus applied potential of electrolyte bath containing $ZnSO_4$ and $Na_2S_2O_3$ with scan speed 25 mv/sec

3.2. Cyclic voltammetry

Figure 3 shows cyclic voltammetry of electrolyte bath at scan speed 25 mv/sec. Cyclic voltammetry (CV) was used to determine the optimal deposition potential of ZnS and study of the corresponding deposition mechanism. It indicates variation of potential with current to find suitable deposing potential of ZnS material. The first and second anodic peak was found at +0.25 V, +0.80 V at scan speed 25 mV/s. Dissolution of sulfide and zinc ions in to the solution has been observed respectively. At that instant, the deposition of ZnS takes place when cathodic potential was reached -0.80 V against Ag/AgCl (Reference Electrode). Therefore, the optimal potential range for deposition of ZnS is -0.8 to -1 V.

3.3. Estimation of layer thickness

Figure 4 shows the deposition time versus thickness of ZnS film.

The thickness of film variation was estimated by using mass difference method:

$$t = \frac{\Delta m}{A \cdot \rho}, \tag{3}$$

where Δm is mass difference of stainless steel substrate before deposition and after deposition, t is thickness of film, A is area of deposition, ρ is density of deposited material. The standard density of ZnS particles was 4.090 g/cm^3. The process of layer formation was found to time dependent. The ZnS particle growth was studied over the range of deposition times from 10 to 40 min. It has been observed that thickness of layer increased up to 20 min, and after that, it was decreased by co-deposition. The optimized thickness of the layer was 3.92 μm at 20 min. The thickness of the ZnS layer was found to be highest at 20 min. The real thickness of the layer will be higher than the calculated values. Because layers may have some porosity, there exists uncertainty in layer thickness.

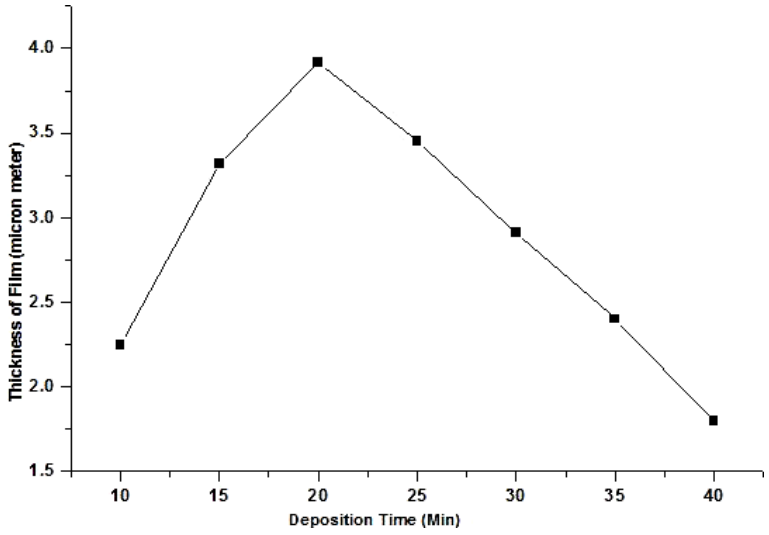

FIG. 4. Deposition time (min) versus thickness of layer

3.4. Effect of complexing agent

In this report triethanolamine (TEA) was used as a complexing agent to prepare ZnS film at optimized time 20 min [14]. The ZnS film deposited at pH 3.5 at different percentage of 0.1 N triethanolamine such as 1, 2, 3, and 4 % of total 80 ml electrolytic bath. The prepared films of ZnS were characterized by using Field Emission Scanning Electron Microscope (FESEM). The SEM image indicated that high dense ZnS filmwas deposited at 4 % TEA if compared to those prepared in the 1 % TEA of complexing agent [14]. It has been observed in Fig. 5. The ZnS film deposited with 4 % TEA was optimized. It showed high dense and good surface coverage of substrate. It can be seen that ZnS film was found densely covered full substrate area if percentage of complexing agent are increased.

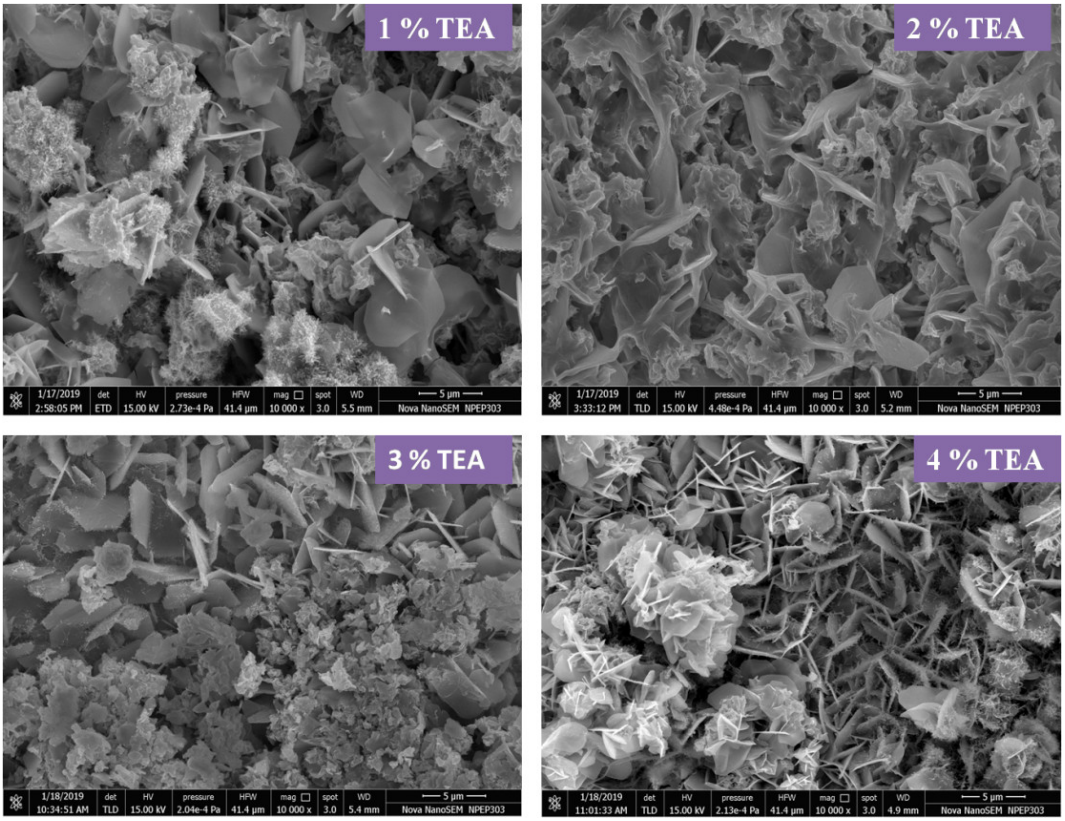

FIG. 5. Scanning electron microscopy image of deposited layer of ZnS particles with complexing agent triethanolamine (TEA) (a) 1 % TEA; (b) 2 % TEA; (c) 3 % TEA; (d) 4 % TEA

3.5. Effect of pH

Figure 6 shows SEM images of deposited of ZnS particle layers with different pH. The SEM was carried out to study the effect of different pH values of solution on surface morphology of ZnS particles. The pH of solution varied from 3.5 to 5; it introduced crystallite defect. It has been observed that two types of particles were found, namely nanorods and lamilar. The average diameter of nanorods was estimated by using image-J software. The nanorods diameter was found to decrease in order to increased pH of solution [15]. It has been shown in Table 1.

The optical absorbance spectra of the ZnS particles by the electrode position method with different pH solution are shown in Fig. 7. The optical absorbance data of the particles were carried out by using UV-Visible spectrophotometer in the wavelength range from 100 to 1100 nm. It is shown that a sharp rise in absorbance occurs between 330 and 360 nm. These are fundamental absorption edges. It is indicated to excitation of electron from valence band to conduction band.

Figure 8 shows optical transmission spectra of ZnS particles deposited by electrode position method with different pH solution [15]. All films showed sharp absorption edges at near 330 nm which correspond to optical band gap of films. It can be observed that average transmission values are 80 % in the wavelength range after 330 nm. The absorption of light in the wavelength region of 330 nm to 360 nm is caused by crystalline defects. The crystalline defects were found to be responsible for reduction in optical transmission. It can be seen that varying pH introduces crystalline defects in ZnS particles as shown in Fig. 6.

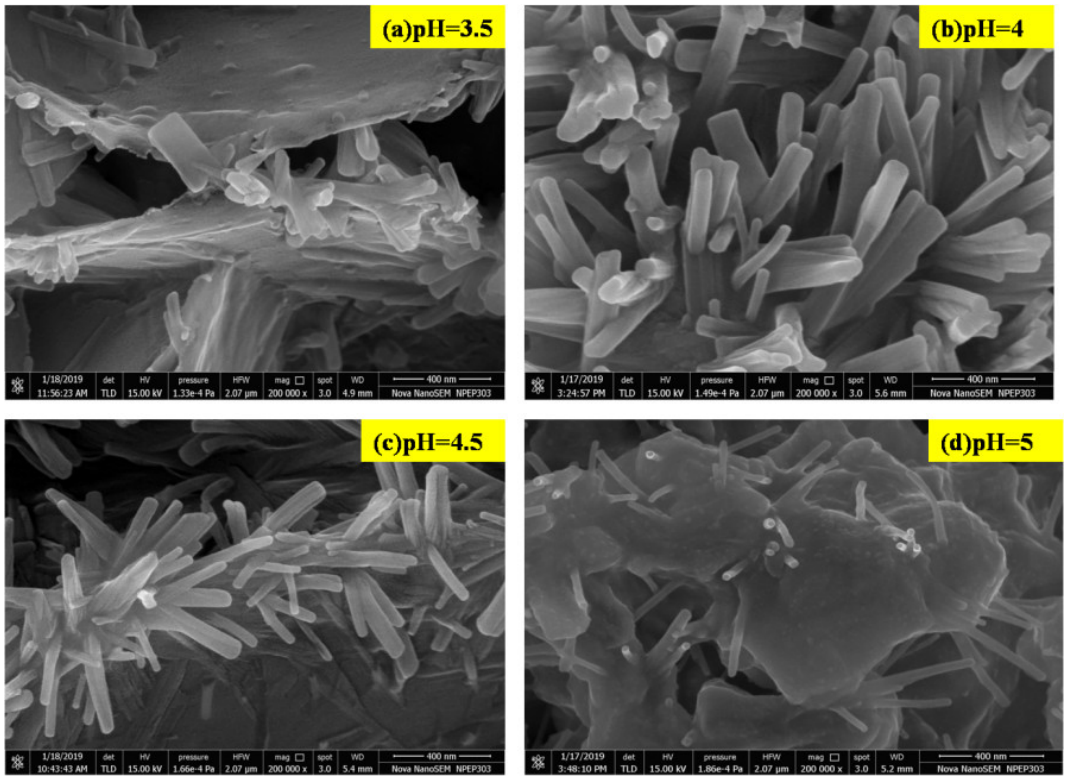

FIG. 6. Scanning electron microscope image of deposited layer of ZnS particles at (a) pH = 3.5; (b) pH = 4; (c) pH = 4.5; (d) pH = 5

TABLE 1. Estimated values of average diameter of nanorods and band gap of ZnS at different pH of bath

Sr. No	pH of solution	Average diameter of nanorod (nm)	Energy Band gap (eV)
1	3.5	160.12 ± 0.5 nm	3.98
2	4	100.15 ± 0.5 nm	3.91
3	4.5	60.10 ± 0.5 nm	3.87
4	5	40.22 ± 0.5 nm	3.74

Figure 9 shows energy band gap of ZnS particles deposited with varying pH of solution from 3.5 to 5. The band gap energies of the deposited particles were calculated with the help of an optical absorption spectrum. i.e. Taucplot. The absorption coefficient (α) was calculated by using equation:

$$\alpha = \frac{\text{Absorbance}}{\text{Thickness of film}}. \tag{4}$$

The optical band gap energy of ZnS particles were calculated by plotting graph $(\alpha h\nu)^2$ versus $h\nu$ [16–19]. The band gaps were determined by the intercept of straight line portion of the $(\alpha h\nu)^2$ versus $h\nu$ graph on the $h\nu$ axis. The direct band gap was calculated to be 3.98 eV and decreased to 3.74 eV after increasing pH of solution. The effect of crystallite defects on band gap of ZnS at different pH of solution as shown in Table 1.

3.6. Effect of deposited layer thickness

The various thicknesses of layer characterized by UV-visible spectrophotometer. Fig. 10 shows optical absorption spectra of ZnS particles deposited by the electrode position method at different thicknesses [20]. The sharp rise of absorption occurs between 300 to 350 nm of thickness range 2400 to 3920 nm.

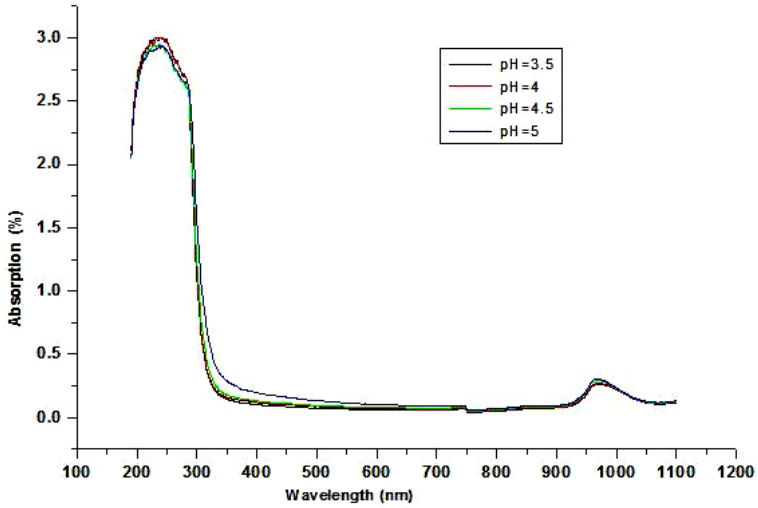

FIG. 7. Optical absorbance spectra of ZnS films deposited at different pH solution

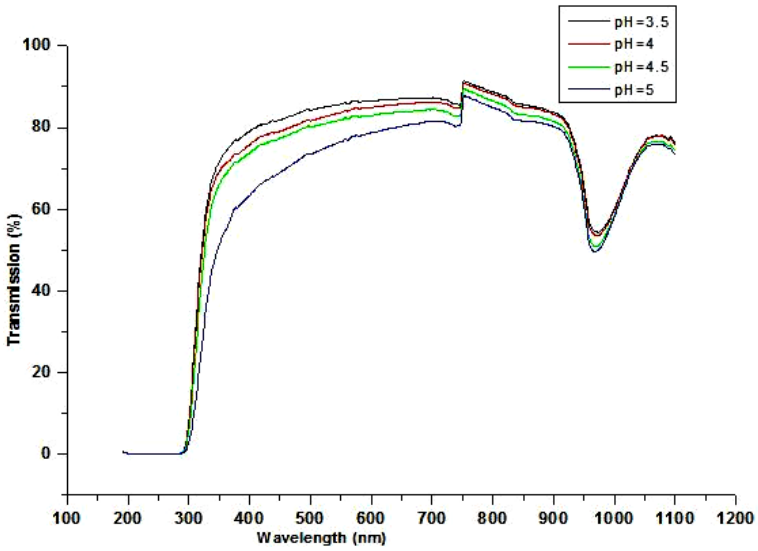

FIG. 8. Optical transmittance spectra of ZnS films deposited at different pH solution

Figure 11 shows transmittance spectra of ZnS particles with various thicknesses. It has been observed that 80 % transmittance occurs for all thickness above wavelengths of 350 nm. The maximum absorption at various layer thicknesses was found to be at wavelengths lower than 350 nm.

Figure 12 shows the optical band gap energies for various particle layer thicknesses. The optical band gap energy of ZnS particles of various thicknesses were calculated by plotting graph $(\alpha h\nu)^2$ versus $h\nu$ [21]. The band gap values varied from 4.10 to 3.78 eV. Of varied thickness 2400 to 3920 nm. It showed band gap energy deceased with increased thickness of layer [22, 23]. The effect of thickness on band gap energy as shown in Table 2.

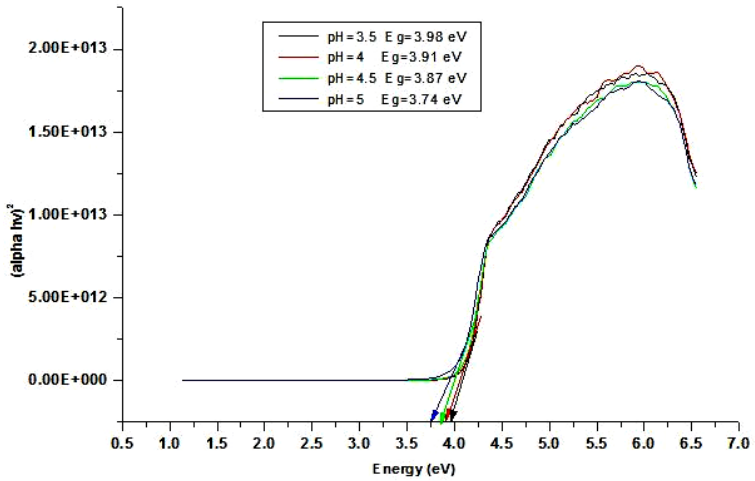

FIG. 9. Energy gap of ZnS films deposited with different pH solution

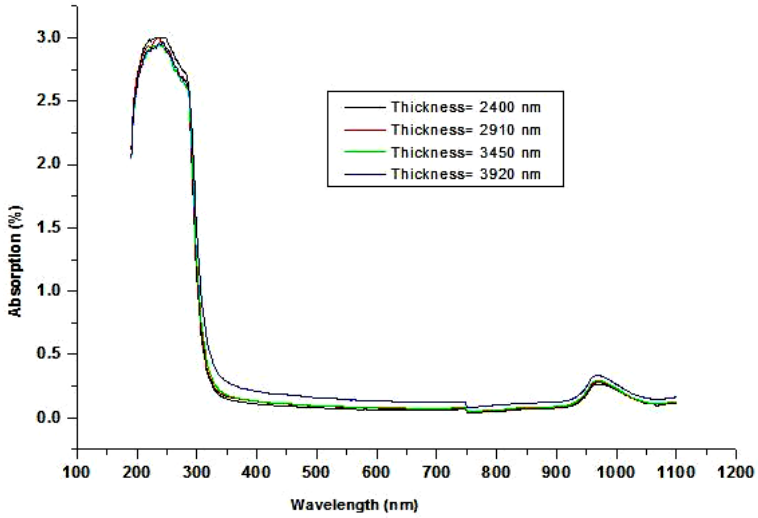

FIG. 10. Optical absorbance spectra of ZnS particles with different thickness

TABLE 2. Estimated values of band gap with different thickness of films

Sr. No.	Thickness of layer (nm)	Band gap energy (eV)
1	2400	4.10
2	2910	3.99
3	3450	3.90
4	3920	3.78

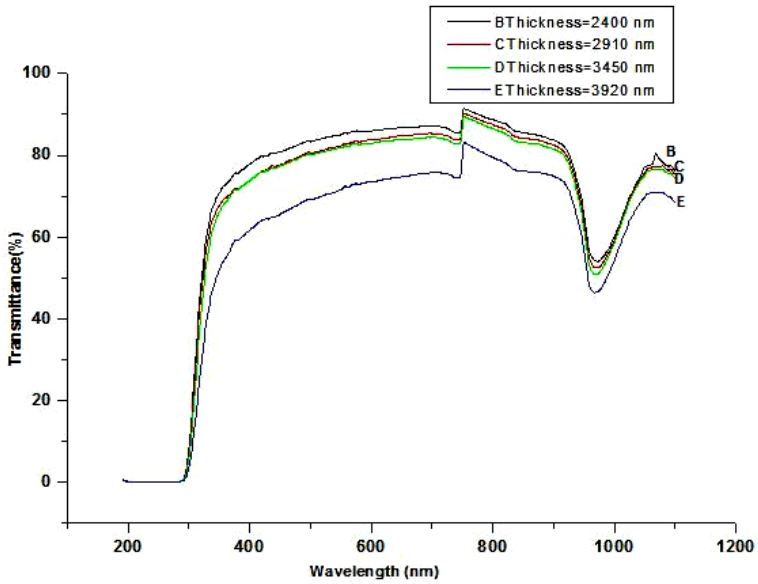

FIG. 11. Transmittance spectra of ZnS particles with different thickness

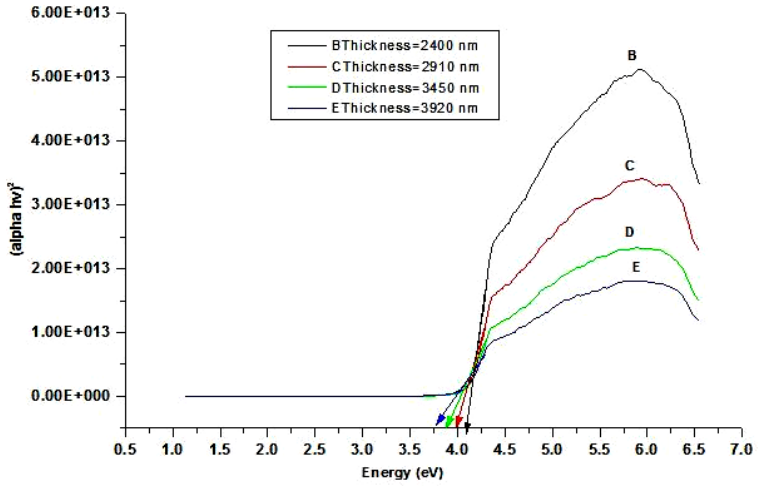

FIG. 12. Energy band gap of ZnS particles with different thickness

3.7. Electrical resistivity

A direct current two point probe technique in air was implemented for characterized the ZnS particles resistivity. The electrical resistivity was estimated by using eq. (3):

$$R = \frac{\rho \cdot L}{dW}, \tag{5}$$

where R – resistance of film, ρ – resistivity of film, L – length of rectangular substrate, dW – element of width.

The resistivity of particles depends on resistance of layer and its thickness. It has been observed that a change in thickness of layer gives variation in electrical resistivity.

The resistivity of various layer thicknesses estimated as shown in Table 3.

It confirmed the resistivity of ZnS particles decreases from $1.782 \cdot 10^6$ to $0.462 \cdot 10^6$ (Ω·cm) as layer thickness increases from 2400 to 3920 nm, due to the improved crystallinity of ZnS particles. The size effect in semiconductor thin films was introduced for this behavior. Fig. 13 shows the variation of resistivity with thickness of ZnS particles.

The ZnS particles deposited on substrate with high concentration of Zn^{2+} ions as compared to S ions and this is n-type ZnS film hence it has been observed in edax spectra as Zn:S =9.24:1.

TABLE 3. Illustrate the variation of electrical resistivity with thickness of ZnS particles layer

Sr.No.	Thickness of layer (nm)	Resistivity (Ω·cm)
1	2400	$1.782 \cdot 10^6$
2	2910	$1.396 \cdot 10^6$
3	3450	$0.868 \cdot 10^6$
4	3920	$0.462 \cdot 10^6$

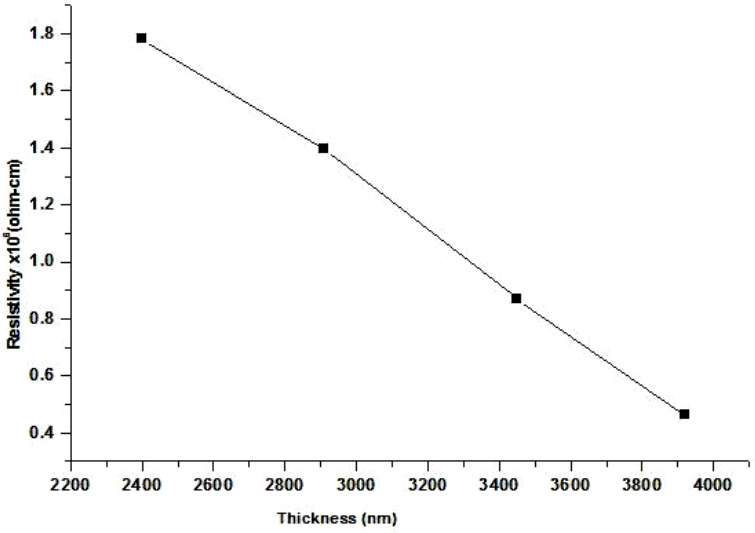

FIG. 13. Variation of resistivity with film thickness of ZnS films

During the growth process of ZnS, not only the Zn and S were found, but also the presence of oxygen appeared, actually there was a significant amount of oxygen present in the ZnS layer. The impure Zn included in deposited layer because ZnS include oxygen element. There is impact of this additional phase on electrical behavior. The resistivity value decreases as the oxygen content is increased in ZnS. It maybe owing to the higher defect existed in ZnS and surface state density existed in the higher oxygen incorporated. The thickness of the layer increases when more oxygen is introduced in ZnS and resistivity will decrease.

4. Conclusion

The ZnS particles were successfully deposited on FTO/stainless steel substrate by an electrode position technique in the presence of triethanolamine as complexing agent. By using scanning electron microscope and UV-Visible spectrophotometer ZnS layers were studied. The SEM images showed that the layer was found good quality and fully substrate coverage at 4 % triethanolamine as compared to film in absence of triethanolamine. The effects of pH on surface morphology, optical properties of ZnS particles were investigated. It was shown that the average crystalline nanorod diameter and band gap decreases with increasing the pH values in range 3.5 to 5. The crystalline nanorod diameter of ZnS particles were found to be between 160.12 – 40.22 nm. The pH values were found to be responsible for crystal defect.The optical band gap values of ZnS particles were found to be 3.98 to 3.74 eV. The thickness of layer was also affected on optical properties.The thickness of layer varied from 2400 to 3920 nm. The optical band gaps were found to range from 4.10 to 3.78 eV. The thickness of layer increases with decreasing band gap energy. The complexing agent, pH of solution and thickness has an important role in controlling morphological and optical properties of the ZnS particles layer. The resistivity of layer was found to thickness dependent. The thickness of layer ranged from 2400 to 3920 nm the resistivity were measured in range $1.782 \cdot 10^6$ to $0.462 \cdot 10^6$ (Ω·cm). It confirmed that the resistivity of layer decreases as layer thickness increases.

Acknowledgements

The authors wish to thank the Physics Research centre M.S.G. College Malegaon camp Malegaon for giving instrument facilities to carry out this research work. Authors also thanks to SAIF IIT Madras and The CIF, Savitribai phule Pune University for providing EDAX and SEM characterization results.

References

[1] Farjami Shayesteh S., Kolahi S., Azizian Kalandarragh Y. Effect of pH on structural and optical properties of ZnS nanoparticles embedded in PVA matrix. *Indian journal of pure and applied physics*, 2013, **51**, P. 780–783.

[2] Aybek A.S., Ruzgar H. Effect of the pH on crystal structure, optical and surface morphological properties of the CdS films deposited by chemical bath deposition. *Chalcogenide Letters*, 2016, **13** (8), P. 339–350.

[3] Guzeldir B., Saglam M., Ates A. Deposition and characterization of CdS, CuS and ZnS thin Films deposited by SILAR method. *Proceedings of the International Congress on Advances in Applied Physics and Materials Science*, Antalya, 2012, **121**, P. 33–35.

[4] Nabiyouni G., Sahraei R. et al. Preparation and characterization of nanostructures thin films grown on glassand n-type si substrates using a newchemical bath deposition technique. *Rev. Adv. Mater. Sci.*, 2011, **27**, P. 52–57.

[5] Echendu, Weerasinghe O.K., et al. Characterization of n-type andp-type ZnS thin layers grown by an electrochemical method. *J. Electron. Mater.*, 2013, **42**, P. 692–700.

[6] Miyawaki T., Ichimura M. Fabrication of ZnS thin films by an improved photochemical deposition method and application to ZnS/SnS heterojunction cells. *Mater. Lett.*, 2007, **61**, P. 4683–4686.

[7] Saravanan Nagalingam, Geok Bee Teh, Rong-FuhLouh, Kai Tung Chee. Cyclic voltammetry studies of cadmium zinc sulfide aqueous solution. *International Journal of the Physical Sciences*, 2011, **6** (31), P. 7166–7170.

[8] Ojo A.A., Dharmadasa I.M. Analysis of the electronic properties of all-electroplated ZnS, CdS and CdTe graded bandgap photovoltaic device configuration. *Sol. Energy*, 2017, **158**, P. 721–727.

[9] Olusola O.I., Madugu M.L., Dharmadasa I.M. Investigating the electronic Properties of multi-junction ZnS/CdS/CdTe gradedband gap solar cells. *Mater. Chem. Phys.*, 2016, **191**, P. 145–150.

[10] Kassim A., Tan W.T., Ho S.M., Saravanan N. Influence of ph on the structural and morphologicalproperties of ZnS thin films. *Anadolu University Journal of Science and Technology A*, 2010, **11** (1), P. 17–22.

[11] Senthil Kumar Vellingiri. Study on physical properties of ZnS thin films prepared by chemical bath deposition. *Asia Pacific Journal of Research*, 2013, **1** (8), P. 5–14.

[12] Chung H.V., Huy P.T., An T.T. Synthesis and opticalproperties of ZnS Nanostructures. *Journal of the Korean Physical Society*, 2008, **52**, 1562.

[13] Acharya S.A., Maheshwari N., et al. Ethylenediamine-mediated wurtzite phase formation in ZnS. *Cryst. Growth Des.*, 2013, **13**, 1369.

[14] Dutta A., Panda S.K., Chaudhuri S. Phase transformation and optical properties of Cu-doped ZnS nanorods. *Journal of Solid State Chemistry*, 2008, **181**, 2332.

[15] Nabiyony G., Sahraei R., et al. Preparation and characterization of nanostructured ZnS thin films grown on glass and n-type Si substrates using a new chemical bath deposition technique. *Rev. Adv. Mater. Sci.*, 2011, **27**, P. 52–57.

[16] Ben Bacha K., Timoumi A., Bitri N., Bouzouitastructural H. Morphological and optical properties of sprayed ZnS thin films on various substrate natures. *Optik*, 2015, **126** (21), P. 3020–3024.

[17] Ghezali K., Mentar L., Boudine B., Azizi A. Electrochemical deposition of ZnS thin films and their structural, morphological and optical properties. *Journal of Electro Analytical Chemistry*, 2017, **794**, P. 212–220.

[18] Azmand A., Kafashan H. Physical and electrochemical properties of electrodeposited undoped and Se-doped ZnS thin films. *Ceramics International*, 2018, **44** (14), P. 17124–17137.

[19] Azmand A., Kafashan H. Al-doped ZnS thin films: physical and electrochemical characterizations. *Journal of Alloys and Compounds*, 2019, **779**, P. 301–313.

[20] Seyed Mostafa Mosavi, Hosein Kafashan. Physical properties of Cd-doped ZnS thin films. *Superlattices and Microstructures*, 2019, **126**, P. 139–149.

[21] Asghar M., Mahmood K., et al. Effect of annealing temperature on the structural and optical properties of ZnS thin films. *Materials Today*, 2015, **2**, P. 5430–5435.

[22] Lopez M.C., Espinos J.P., et al. Growth of ZnS thin films obtained by chemical spray pyrolysis: the influence of precursors. *Journal of Crystal Growth*, 2005, **285** (1–2), P. 66–75.

[23] Hernandez-Fenollosa M.A., Lopez M.C., et al. Role of precursorson morphology and optical properties of ZnS thin films prepared by chemical spray pyrolysis. *Thin Solid Films*, 2008, **516**, P. 1622–1625.